

AFB in High Invariant-Mass Drell-Yan Implications for SMEFT Fits

Yingsheng Huang

Northwestern U. & Argonne

In collaboration with:

Radja Boughezal and Frank Petriello



Northwestern
University

arxiv: 2304.11142

May 8th @ Phenomenology 2023



TABLE OF CONTENTS

1 Introduction

2 SMEFT Operators

3 AFB in NC Drell-Yan

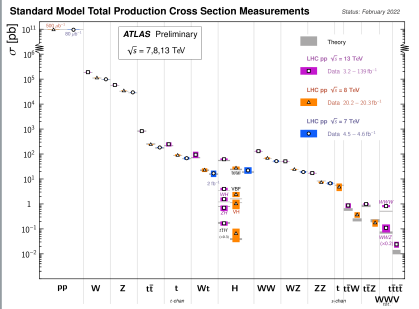
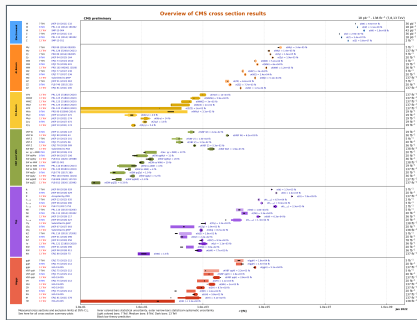
4 Results

- Data sets
- Linear contributions only
- Quadratic contributions

5 Conclusions

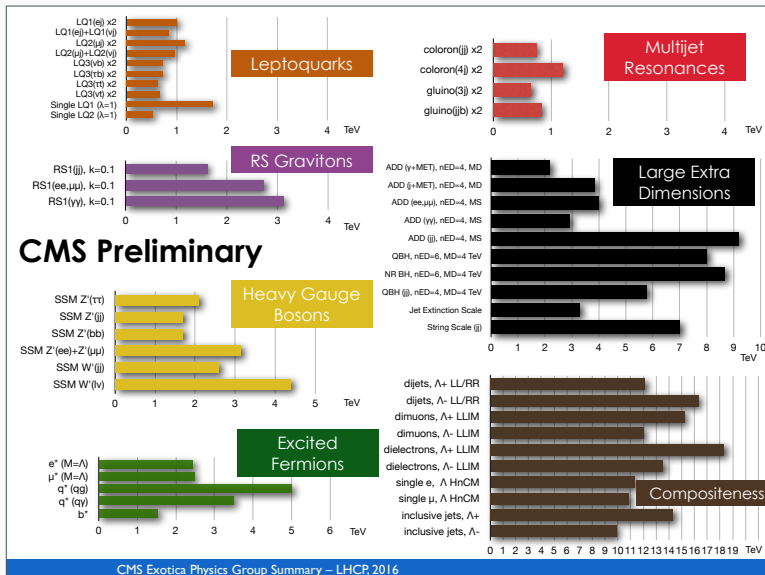
STATUS OF THE SM

Examples:



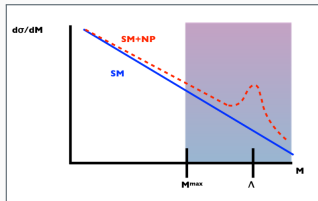
Remarkable agreement between theory predictions and the experiment measurements!

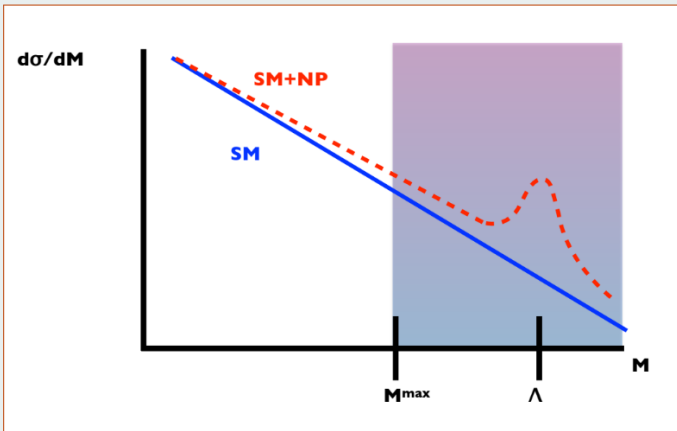
BSM SEARCHES



SMEFT a model-independent approach

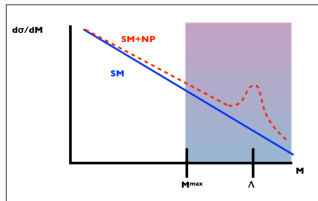
- No BSM particle found
- Calls for precision test of SM





SMEFT a model-independent approach

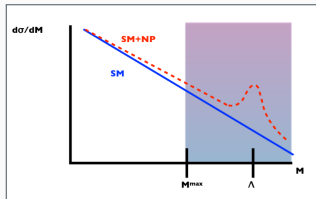
- No BSM particle found
- Calls for precision test of SM



- Standard Model Effective Field Theory (SMEFT)
 - SM particles
 - all possible operators satisfying symmetries of the SM
 - power counting: new physics scale Λ
 - Model independent

SMEFT a model-independent approach

- No BSM particle found
- Calls for precision test of SM

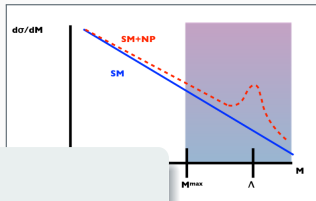


- Standard Model Effective Field Theory (SMEFT)
 - SM particles
 - all possible operators satisfying symmetries of the SM
 - power counting: new physics scale Λ
 - Model independent
- Lagrangian of SMEFT

$$\mathcal{L}_{\text{SMEFT}} = \mathcal{L}_{\text{SM}} + \boxed{\frac{1}{\Lambda^2} \sum C_6 \mathcal{O}_6} + \boxed{\frac{1}{\Lambda^4} \sum C_8 \mathcal{O}_8} + \dots$$

- ▶ \mathcal{L}_6 : 76 B-preserving Lagrangian terms, 2499 parameters [Grzadkowski et al. 2010](#)
- ▶ \mathcal{L}_8 : 1031 Lagrangian terms, 44807 parameters [Murphy 2020; Li et al. 2021](#)

- No BSM particle found
- Calls for precision test of SM



In this talk:

- Standard Model
 - SM parameters
 - all possible terms
 - power corrections
 - Model independent
- Warsaw basis for dimension-6
- No odd dimensions
- Four-fermion sector
- Lagrangian of SMEFT

$$\mathcal{L}_{\text{SMEFT}} = \mathcal{L}_{\text{SM}} + \boxed{\frac{1}{\Lambda^2} \sum C_6 \mathcal{O}_6} + \boxed{\frac{1}{\Lambda^4} \sum C_8 \mathcal{O}_8} + \dots$$

- \mathcal{L}_6 : 76 B-preserving Lagrangian terms, 2499 parameters [Grzadkowski et al. 2010](#)
- \mathcal{L}_8 : 1031 Lagrangian terms, 44807 parameters [Murphy 2020; Li et al. 2021](#)

- Low-energy constraints, weaker than those provided by Drell-Yan at the LHC [Falkowski, González-Alonso, and Mimouni 2017](#); [Boughezal, Petriello, and Wiegand 2021](#)
- Dimension-8 level:
 - dilepton invariant mass, sensitivity of operators at high energy [Boughezal, Mereghetti, and Petriello 2021](#)
 - transverse momentum distribution, help distinguish between possible UV completions [Boughezal YH, and Petriello 2022](#).
- QCD and electroweak corrections to the SMEFT contributions up to NLO [Dawson, Giardino, and Ismail 2019](#); [Dawson and Giardino 2021](#)
- Global fits of available high invariant mass distributions [Allwicher et al. 2022](#)

- Low-energy constraints, weaker than those provided by Drell-Yan at the LHC [Falkowski, González-Alonso, and Mimouni 2017](#); [Boughezal, Petriello, and Wiegand 2021](#)
- Dimension-8 level:
 - dilepton invariant mass, sensitivity of operators at high energy [Boughezal, Mereghetti, and Petriello 2021](#)
 - transverse momentum distribution, help distinguish between possible UV completions [Boughezal YH, and Petriello 2022](#).
- QCD and electroweak corrections to the SMEFT contributions up to NLO [Dawson, Giardino, and Ismail 2019](#); [Dawson and Giardino 2021](#)
- Global fits of available high invariant mass distributions [Allwicher et al. 2022](#) talk by Allwicher

- Low-energy constraints, weaker than those provided by Drell-Yan at the LHC [Falkowski, González-Alonso, and Mimouni 2017](#); [Boughezal, Petriello, and Wiegand 2021](#)
- Dimension-8 level:
 - dilepton invariant mass, sensitivity of operators at high energy [Boughezal, Mereghetti, and Petriello 2021](#)
 - transverse momentum distribution, help distinguish between possible UV completions [Boughezal YH, and Petriello 2022](#).
- QCD and electroweak corrections to the SMEFT contributions up to NLO [Dawson, Giardino, and Ismail 2019](#); [Dawson and Giardino 2021](#)
- Global fits of available high invariant mass distributions [Allwicher et al. 2022](#)
- Drell-Yan invariant mass distributions can only constrain a limited number of combinations of four-fermion Wilson coefficients (**flat direction**) [Alte, König, and Shepherd 2019](#); [Boughezal, Petriello, and Wiegand 2020](#)
- Future colliders such as the electron-ion collider (EIC) can remove these degeneracies [Boughezal, Petriello, and Wiegand 2020](#)

talk by Allwicher

- Low-energy constraints, weaker than those provided by Drell-Yan at the LHC [Falkowski, González-Alonso, and Mimouni 2017](#); [Boughezal, Petriello, and Wiegand 2021](#)
- Dimension-8 level:
 - dilepton invariant mass, sensitivity of operators at high energy [Boughezal, Mereghetti, and Petriello 2021](#)

Complement [dilepton invariant mass dist.](#) ($d\sigma/dm$)

- QC with [forward-backward asymmetry \(AFB\) data](#)
[Day](#) in neutral current Drell-Yan process
- Global fit to [Drell-Yan invariant mass distributions](#) can only constrain a limited number of combinations of four-fermion Wilson coefficients ([flat direction](#)) [Alte, König, and Shepherd 2019](#); [Boughezal, Petriello, and Wiegand 2020](#)
- Future colliders such as the electron-ion collider (EIC) can remove these degeneracies [Boughezal, Petriello, and Wiegand 2020](#)

Why only four-fermion?

- Study scaling of cross sections in high energy limit (s, v)
 - Only show some examples for each category
 - q, l : left-handed fermion doublets
 e, u, d : right-handed fermion singlets
 - ϕ : Higgs doublet
-

$$\mathcal{L}_{\psi^2 X^2 \phi}$$

$$\mathcal{L}_{\psi^2 \phi^2 D}$$

$$\mathcal{L}_{\psi^4}$$

$$\frac{C_{eB}}{\Lambda^2} \bar{l} \sigma^{\mu\nu} B_{\mu\nu} \phi e$$

$$\frac{C_{uW}}{\Lambda^2} \bar{q} \sigma^{\mu\nu} \tau^I W_{\mu\nu}^I \phi u$$

Dipole coupling

assume massless fermion

$$\sim \mathcal{O}(v^2 s / \Lambda^4)$$

$$\frac{C_{Hl}^{(1)}}{\Lambda^2} \phi^\dagger \overleftrightarrow{D}^\mu \phi \bar{l} \gamma_\mu l$$

$$\frac{C_{Hu}}{\Lambda^2} \phi^\dagger \overleftrightarrow{D}^\mu \phi \bar{u} \gamma_\mu u$$

Z-vertex corrections

$$\frac{C_{lq}^{(1)}}{\Lambda^2} \bar{l} \gamma^\mu l q \gamma_\mu q$$

$$\frac{C_{ld}}{\Lambda^2} \bar{l} \gamma^\mu l d \gamma_\mu d$$

Four-fermion interactions

$$\sim \mathcal{O}(s / \Lambda^2)$$

- Study scaling of cross sections in high energy limit (s, v)
- Only show some examples for each category
- q, l : left-handed fermion doublets
 e, u, d : right-handed fermion singlets
- ϕ : Higgs doublet

$$\mathcal{L}_{\psi^2 X^2}$$

Best constrained by high $m_{\ell\ell}$ data

$$b^4$$

$$\frac{C_{eB}}{\Lambda^2} \bar{l} \sigma^{\mu\nu} B_{\mu\nu} \phi e$$

$$\frac{C_{Hl}^{(1)}}{\Lambda^2} \phi^\dagger \overleftrightarrow{D}^\mu \phi \bar{l} \gamma_\mu l$$

$$\frac{C_{lq}^{(1)}}{\Lambda^2} \bar{l} \gamma^\mu l q \gamma_\mu q$$

$$\frac{C_{uW}}{\Lambda^2} \bar{q} \sigma^{\mu\nu} \tau^I W_{\mu\nu}^I \phi u$$

$$\frac{C_{Hu}}{\Lambda^2} \phi^\dagger \overleftrightarrow{D}^\mu \phi \bar{u} \gamma_\mu u$$

$$\frac{C_{ld}}{\Lambda^2} \bar{l} \gamma^\mu l d \gamma_\mu d$$

Dipole coupling

Z-vertex corrections

Four-fermion interactions

assume massless fermion

$$\sim \mathcal{O}(v^2 s / \Lambda^4)$$

$$\sim \mathcal{O}(v^2 / \Lambda^2)$$

$$\sim \mathcal{O}(s / \Lambda^2)$$

RELEVANT FOUR-FERMION OPERATORS

$\mathcal{O}_{lq}^{(1)}$	$(\bar{l}\gamma^\mu l)(\bar{q}\gamma_\mu q)$	\mathcal{O}_{lu}	$(\bar{l}\gamma^\mu l)(\bar{u}\gamma_\mu u)$
$\mathcal{O}_{lq}^{(3)}$	$(\bar{l}\gamma^\mu \tau^I l)(\bar{q}\gamma_\mu \tau^I l q)$	\mathcal{O}_{ld}	$(\bar{l}\gamma^\mu l)(\bar{d}\gamma_\mu d)$
\mathcal{O}_{eu}	$(\bar{e}\gamma^\mu e)(\bar{u}\gamma_\mu u)$	\mathcal{O}_{qe}	$(\bar{q}\gamma^\mu q)(\bar{e}\gamma_\mu e)$
\mathcal{O}_{ed}	$(\bar{e}\gamma^\mu e)(\bar{d}\gamma_\mu d)$		

Structure of the SMEFT cross section

$$\frac{d\sigma}{dm_{\ell\ell}dc_\theta^*} = \frac{d\sigma_{\text{SM}}}{dm_{\ell\ell}dc_\theta^*} + \sum_i \frac{a_i^{(6)}(m_{\ell\ell}, c_\theta^*)}{\Lambda^2} C_i^{(6)} + \sum_{i,j} \frac{b_{ij}^{(6)}(m_{\ell\ell}, c_\theta^*)}{\Lambda^4} C_i^{(6)} C_j^{(6)}$$

- $c_\theta^* \equiv \cos \theta^*$
- SM: NLO in QCD, NLL Sudakov logs through $\mathcal{O}(\alpha_s)$
- a_i, b_{ij} terms: LO in QCD
- No dim-8 operators

AFB in neutral current Drell-Yan

AFB

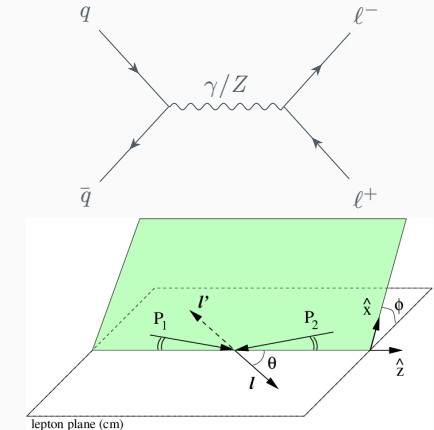
$$A_{\text{FB}} = \frac{\sigma_F - \sigma_B}{\sigma_F + \sigma_B}$$

- depends on Collins-Soper angle θ^*
- σ_F : forward ($\cos \theta^* > 0$)
- σ_B : backward ($\cos \theta^* < 0$)

Collins-Soper angle [Collins and Soper 1977](#)

$$\cos \theta^* = \frac{2(P_1^+ P_2^- - P_1^- P_2^+)}{\sqrt{Q^2(Q^2 + Q_T^2)}} \quad (\text{hadron C.M.})$$

- angle between the incoming quark and the outgoing lepton (negatively charged) in the dilepton rest frame



SMEFT corrections to AFB

$$\begin{aligned}
 A_{\text{FB}}^{\text{SMEFT}} &= A_{\text{FB}} - A_{\text{FB}}^{\text{SM}} \\
 &= \sum_i \frac{C_i^{(6)}}{\Lambda^2} \frac{\sigma_{\text{SM}} \Delta a_i^{(6)} - a_i^{(6)} \Delta \sigma_{\text{SM}}}{\sigma_{\text{SM}}^2} \\
 &\quad + \sum_{ij} \frac{C_i^{(6)} C_j^{(6)}}{\Lambda^4} \frac{\left(a_i^{(6)}\right)^2 \Delta \sigma_{\text{SM}} - a_i^{(6)} \Delta a_i^{(6)} \Delta \sigma_{\text{SM}} - b_{ij}^{(6)} \sigma_{\text{SM}} \Delta \sigma_{\text{SM}} + \Delta b_{ij}^{(6)} \sigma_{\text{SM}}^2}{\sigma_{\text{SM}}^3}
 \end{aligned}$$

- $\sigma \equiv \sigma_F + \sigma_B, \Delta\sigma \equiv \sigma_F - \sigma_B$
- Expansion up to $\mathcal{O}(1/\Lambda^4)$, including dim-6 **linear** and **quadratic** contributions

COMBINATIONS OF WILSON COEFFICIENTS & FLAT DIRECTION

LO SMEFT contributions to partonic cross section in high energy limit

$$\frac{d\sigma^x}{dm_{ll}^2 dY dc_\theta^*} \sim \frac{1}{\Lambda^2} \frac{A_1^x \hat{u}^2 + A_2^x \hat{t}^2}{\hat{s}^2} + \frac{1}{\Lambda^4} (B_1^x \hat{u}^2 + B_2^x \hat{t}^2)$$

- x : partonic channel u or d
- A_i^x : linear in $C_i^{(6)}$; B_i^x : quadratic in $C_i^{(6)}$; does not depend on kinematic variables
- $\hat{t} = -\frac{\hat{s}}{2}(1 - c_\theta^*)$, $\hat{u} = -\frac{\hat{s}}{2}(1 + c_\theta^*)$
- $d\sigma/dm$ is only sensitive to $A_1 + A_2$, A_{FB} is sensitive to $A_1 - A_2$

COMBINATIONS OF WILSON COEFFICIENTS & FLAT DIRECTION

LO SMEFT contributions to partonic cross section in high energy limit

$$\frac{d\sigma^x}{dm_{ll}^2 dY dc_\theta^*} \sim \frac{1}{4\Lambda^2} \left[A^x (1 + c_\theta^{*2}) + 2\Delta A^x c_\theta^* \right] + \frac{s^2}{4\Lambda^4} \left[B^x (1 + c_\theta^{*2}) + 2\Delta B^x c_\theta^* \right]$$

- x : partonic channel u or d
- A_i^x : linear in $C_i^{(6)}$; B_i^x : quadratic in $C_i^{(6)}$; does not depend on kinematic variables
- $A^x = A_1^x + A_2^x$, $\Delta A^x = A_1^x - A_2^x$; $B^x = B_1^x + B_2^x$, $\Delta B^x = B_1^x - B_2^x$
- $d\sigma/dm$ is only sensitive to $A_1 + A_2$, A_{FB} is sensitive to $A_1 - A_2$

COMBINATIONS OF WILSON COEFFICIENTS & FLAT DIRECTION

LO SMEFT contributions to partonic cross section in high energy limit

$$\frac{d\sigma^x}{dm_{ll}^2 dY dc_\theta^*} \sim \frac{1}{4\Lambda^2} \left[A^x (1 + c_\theta^{*2}) + 2\Delta A^x c_\theta^* \right] + \frac{s^2}{4\Lambda^4} \left[B^x (1 + c_\theta^{*2}) + 2\Delta B^x c_\theta^* \right]$$

- x : partonic channel u or d
- A_i^x : linear in $C_i^{(6)}$; B_i^x : quadratic in $C_i^{(6)}$; does not depend on kinematic variables
- $A^x = A_1^x + A_2^x$, $\Delta A^x = A_1^x - A_2^x$; $B^x = B_1^x + B_2^x$, $\Delta B^x = B_1^x - B_2^x$
- $d\sigma/dm$ is only sensitive to $A_1 + A_2$, A_{FB} is sensitive to $A_1 - A_2$
- dependence on Wilson coefficients

$$A_1^u = A_1^u(C_{eu}, C_{lq}^{(1)}, C_{lq}^{(3)}),$$

$$A_1^d = A_1^d(C_{ed}, C_{lq}^{(1)}, C_{lq}^{(3)}),$$

$$A_2^u = A_2^u(C_{lu}, C_{qe}),$$

$$A_2^d = A_2^d(C_{ld}, C_{qe}).$$

COMBINATIONS OF WILSON COEFFICIENTS & FLAT DIRECTION

- $d\sigma/dm$ is only sensitive to $A_1 + A_2$, A_{FB} is sensitive to $A_1 - A_2$
- dependence on Wilson coefficients

$$A_1^u = A_1^u(C_{eu}, C_{lq}^{(1)}, C_{lq}^{(3)}),$$

$$A_1^d = A_1^d(C_{ed}, C_{lq}^{(1)}, C_{lq}^{(3)}),$$

$$A_2^u = A_2^u(C_{lu}, C_{qe}),$$

$$A_2^d = A_2^d(C_{ld}, C_{qe}).$$

flat direction: same combination of $C_i^{(6)}$ in both u & d channels

$d\sigma/dm: A_1^x + A_2^x$

AFB: $A_1^x - A_2^x$

DATA SETS FOR FITS

No.	Exp.	\sqrt{s}	Obs.	Lumi. [fb $^{-1}$]	m_{ll}^{low} [GeV]
I	ATLAS ¹	8 TeV	$d\sigma/dm$	20.3	116 – 1000
II	CMS ²	13 TeV	$d\sigma/dm$	137 (ee)	200 – 2210 (ee)
				140 ($\mu\mu$)	210 – 2290 ($\mu\mu$)
III	CMS ³	8 TeV	A_{FB}^*	19.7	120 – 500
IV	CMS ⁴	13 TeV	A_{FB}	138	170 – 1000

- Experimental statistics & systematic uncertainties included, no correlation across date sets
- NNPDF 3.1 NNLO
- PDF & scale uncertainties for SM included in the theory side
- Envelope btw. 7 scale variations

$$\frac{1}{2} \leq \mu_{R,F}/\mu_0 \leq 2, \quad \frac{1}{2} \leq \mu_R/\mu_F \leq 2.$$

DATA SETS FOR FITS

No.	Exp.	\sqrt{s}	Obs.	Lumi. [fb $^{-1}$]	m_{ll}^{low} [GeV]
I	ATLAS ¹	8 TeV	d σ /dm	20.3	116 – 1000
II	CMS ²	13 TeV	d σ /dm	137 (ee)	200 – 2210 (ee)

II Perform χ^2 fits for both single data sets and globally

$$\chi^2 = \sum_{i,j}^{\# \text{of bins}} \frac{(\sigma_i^{\text{SM}} - \sigma_i^{\text{SMEFT}})(\sigma_j^{\text{SM}} - \sigma_j^{\text{SMEFT}})}{\Delta \sigma_{ij}^2}$$

- Ex ac
- NN
- PDF & scale uncertainties for SM included in the theory side
- Envelope btw. 7 scale variations

$$\frac{1}{2} \leq \mu_{R,F}/\mu_0 \leq 2, \quad \frac{1}{2} \leq \mu_R/\mu_F \leq 2.$$

Linear contributions only

Adopt 4 example combinations of Wilson coefficients from

Boughezal, Petriello and Wiegand, 2004.00748

LINEAR CONTRIBUTIONS ONLY

Structure of the SMEFT cross section

$$\frac{d\sigma}{dm_{\ell\ell} dc_\theta^*} = \frac{d\sigma_{\text{SM}}}{dm_{\ell\ell} dc_\theta^*} + \sum_i \frac{a_i^{(6)}(m_{\ell\ell}, c_\theta^*)}{\Lambda^2} C_i^{(6)} + \sum_{i,j} \frac{b_{ij}^{(6)}(m_{\ell\ell}, c_\theta^*)}{\Lambda^4} C_i^{(6)} C_j^{(6)}$$

SMEFT corrections to AFB

$$A_{\text{FB}}^{\text{SMEFT}} = A_{\text{FB}} - A_{\text{FB}}^{\text{SM}}$$
$$= \sum_i \frac{C_i^{(6)}}{\Lambda^2} \frac{\sigma_{\text{SM}} \Delta a_i^{(6)} - a_i^{(6)} \Delta \sigma_{\text{SM}}}{\sigma_{\text{SM}}^2}$$
$$+ \sum_{ij} \frac{C_i^{(6)} C_j^{(6)}}{\Lambda^4} \frac{\left(a_i^{(6)}\right)^2 \Delta \sigma_{\text{SM}} - a_i^{(6)} \Delta a_i^{(6)} \Delta \sigma_{\text{SM}} - b_{ij}^{(6)} \sigma_{\text{SM}} \Delta \sigma_{\text{SM}} + \Delta b_{ij}^{(6)} \sigma_{\text{SM}}^2}{\sigma_{\text{SM}}^3}$$

CASE I C_{eu} , C_{ed} and C_{qe}

- Contributions from $A_1^u(C_{eu})$, $A_1^d(C_{ed})$, $A_2^{u/d}(C_{qe})$
- Conditions for the cross section to vanish after integration over c_θ^* for each channel

$$u : C_{qe} = -C_{eu} \frac{Q_u e^2 - g_Z^2 g_L^u g_R^e}{Q_u e^2 - g_Z^2 g_R^e g_R^u},$$

$$d : C_{qe} = -C_{ed} \frac{Q_d e^2 - g_Z^2 g_L^d g_R^e}{Q_d e^2 - g_Z^2 g_R^e g_R^d},$$

the SM left-handed and right-handed fermion couplings [Denner 1993](#):

$$g_L^f = I_3^f - Q_f s_W^2, \quad g_R^f = -Q_f s_W^2.$$

- These conditions are simultaneously satisfied when

$$C_{ed}^{(1)} \equiv C_{ed} = C_{eu} \frac{Q_u e^2 - g_Z^2 g_L^u g_R^e}{Q_u e^2 - g_Z^2 g_R^e g_R^u} \frac{Q_d e^2 - g_Z^2 g_R^e g_R^d}{Q_d e^2 - g_Z^2 g_L^d g_R^e}$$

CASE I C_{eu} , C_{ed} and C_{qe}

- Contributions from $A_1^u(C_{eu})$, $A_1^d(C_{ed})$, $A_2^{u/d}(C_{qe})$
- Conditions for the cross section to vanish after integration over c_θ^* for each channel

$d\sigma/dm$

- up-quark channel: $A_1^u(C_{eu}) + A_2^u(C_{qe})$
- down-quark channel: $A_1^d(C_{ed}^{(1)}) + A_2^u(C_{qe})$
- same linear combination of C_{eu} & C_{qe}

the SM left

er 1993:

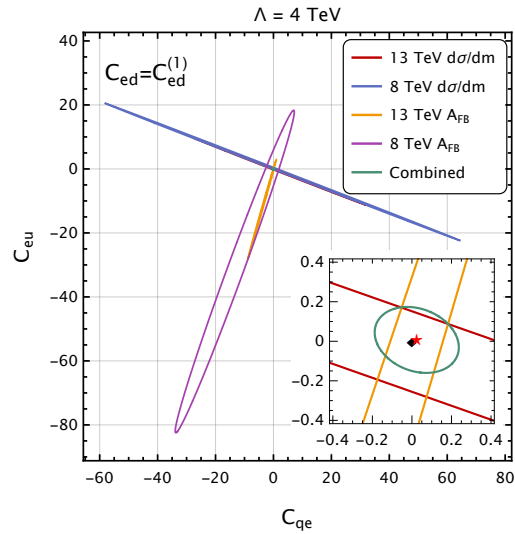
Same for AFB

- These conditions are simultaneously satisfied when

$$C_{ed}^{(1)} \equiv C_{ed} = C_{eu} \frac{Q_u e^2 - g_Z^2 g_L^u g_R^e}{Q_u e^2 - g_Z^2 g_R^e g_R^u} \frac{Q_d e^2 - g_Z^2 g_R^e g_R^d}{Q_d e^2 - g_Z^2 g_L^d g_R^e}$$

CASE I C_{eu} , C_{ed} and C_{qe}

- $C_{ed} = C_{ed}^{(1)}$
⇒ SMEFT corrections vanish in the limit $s \gg M_Z^2$
- both $d\sigma/dm$ and AFB exhibit flat directions
- nearly orthogonal flat directions
- AFB improves fit



CASE II C_{eu} , C_{ed} and $C_{lq}^{(1)}$

- Contributions from $A_1^u(C_{eu}, C_{lq}^1)$, $A_1^d(C_{ed}, C_{lq}^1)$
- Conditions for the cross section to vanish after integration over c_θ^* for each channel

$$u : C_{lq}^{(1)} = -C_{eu} \frac{Q_u e^2 - g_Z^2 g_R^u g_R^e}{Q_u e^2 - g_Z^2 g_L^e g_L^u},$$

$$d : C_{lq}^{(1)} = -C_{ed} \frac{Q_d e^2 - g_Z^2 g_R^d g_R^e}{Q_d e^2 - g_Z^2 g_L^e g_L^d},$$

- These conditions are simultaneously satisfied when

$$C_{ed}^{(2)} \equiv C_{ed} = C_{eu} \frac{Q_u e^2 - g_Z^2 g_R^u g_R^e}{Q_u e^2 - g_Z^2 g_L^e g_L^u} \frac{Q_d e^2 - g_Z^2 g_L^e g_L^d}{Q_d e^2 - g_Z^2 g_R^d g_R^e}.$$

CASE II C_{eu} , C_{ed} and $C_{lq}^{(1)}$

- Contributions from $A_1^u(C_{eu}, C_{lq}^1)$, $A_1^d(C_{ed}, C_{lq}^1)$
- Conditions for the cross section to vanish after integration over c_θ^* for each channel

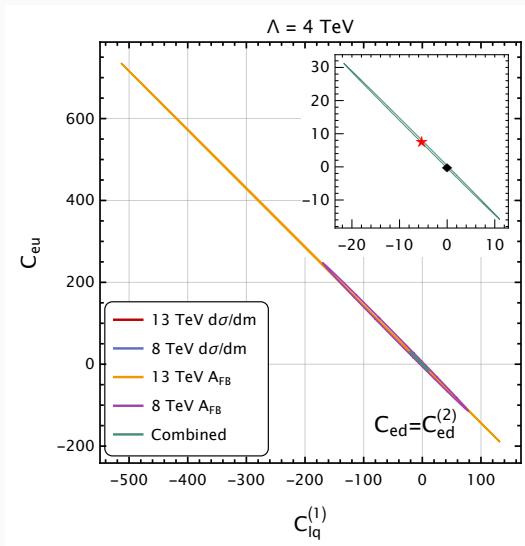
Only A_1 contributes, no difference
between $d\sigma/dm$ and AFB in terms of
dependence in $C^{(6)}$

- These conditions are simultaneously satisfied when

$$C_{ed}^{(2)} \equiv C_{ed} = C_{eu} \frac{Q_u e^2 - g_Z^2 g_R^u g_R^e}{Q_u e^2 - g_Z^2 g_L^e g_L^u} \frac{Q_d e^2 - g_Z^2 g_L^e g_L^d}{Q_d e^2 - g_Z^2 g_R^d g_R^e}.$$

CASE II C_{eu} , C_{ed} and $C_{lq}^{(1)}$

- $C_{ed} = C_{ed}^{(2)}$
- both $d\sigma/dm$ and AFB exhibit flat directions
- pointing at the same direction
- no improvement from AFB



CASE III C_{qe} and $C_{lq}^{(1)}$

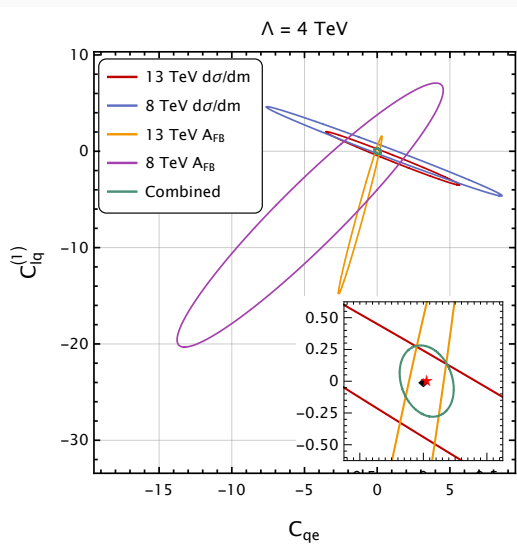
- up-quark channel:

$$C_{lq}^{(1)} = -C_{qe} \frac{Q_u e^2 - g_Z^2 g_L^u g_R^e}{Q_u e^2 - g_Z^2 g_L^e g_L^u}$$

- down-quark channel:

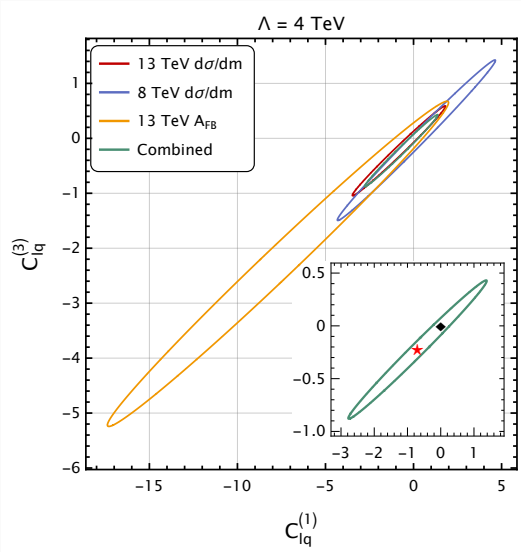
$$C_{lq}^{(1)} = -C_{qe} \frac{Q_d e^2 - g_Z^2 g_L^d g_R^e}{Q_u e^2 - g_Z^2 g_L^e g_L^d}$$

- two channels do not have a common solution \Rightarrow no flat direction
- $d\sigma/dm$ & AFB pointing in opposite directions
- AFB improves fit



CASE IV $C_{lq}^{(1)}$ and $C_{lq}^{(3)}$

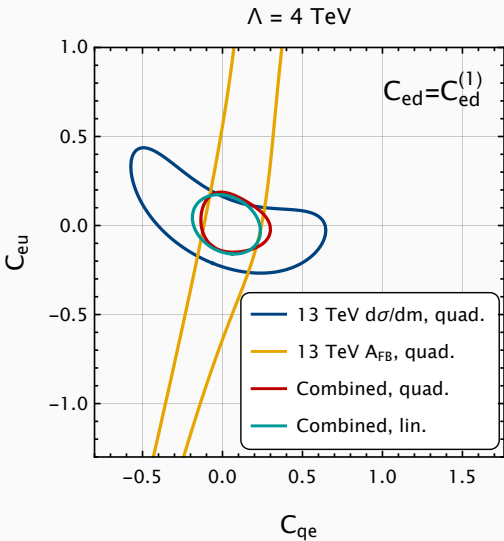
- up-quark channel:
depends on combination
 $C_{lq}^{(1)} + C_{lq}^{(3)}$
- down-quark channel:
depends on combination
 $C_{lq}^{(1)} - C_{lq}^{(3)}$
- no flat direction
- no improvement from AFB



Quadratic contributions

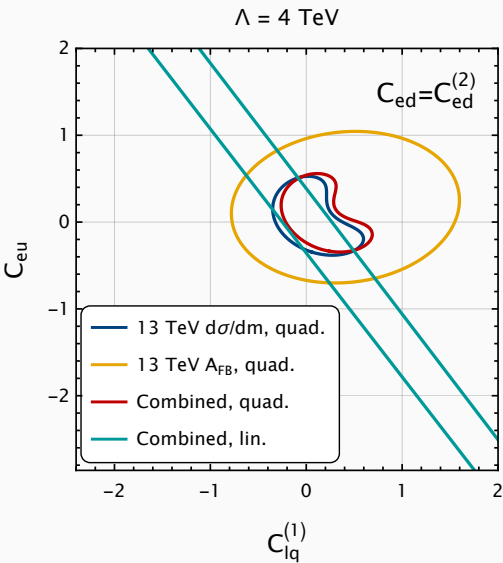
CASE I C_{eu} , C_{ed} and C_{qe}

- $C_{ed} = C_{ed}^{(1)}$
- Quadratic contributions break degeneracies for single measurement
- AFB cancels degeneracies from $d\sigma/dm$ with linear terms only
- Quadratic contributions do not improve the combined fit significantly



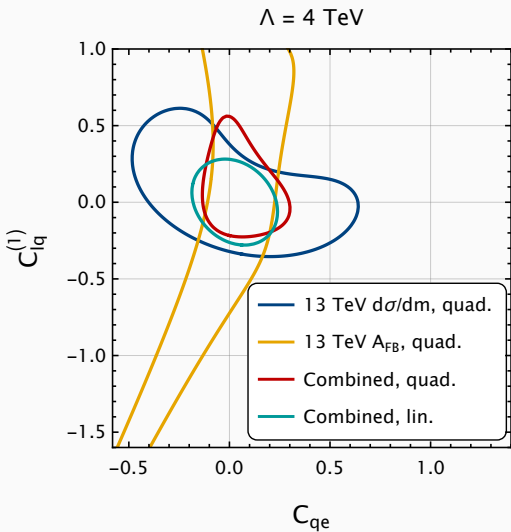
CASE II C_{eu} , C_{ed} and $C_{lq}^{(1)}$

- $C_{ed} = C_{ed}^{(2)}$
- Quadratic contributions break degeneracies for single measurement
- AFB does not cancel degeneracies from $d\sigma/dm$ with linear terms only, combined fit still exhibit flat direction
- Quadratic contributions improve the combined fit significantly



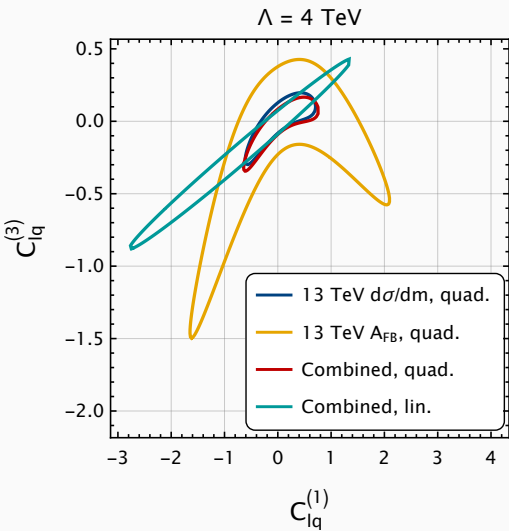
CASE III C_{qe} and $C_{lq}^{(1)}$

- no flat directions at linear order, strong correlation between C_{qe} and $C_{lq}^{(1)}$
- Quadratic contributions reduce correlation for single measurement
- Combining AFB & $d\sigma/dm$ reduces correlation with linear terms only
- Little differences btw. linear and quadratic fits

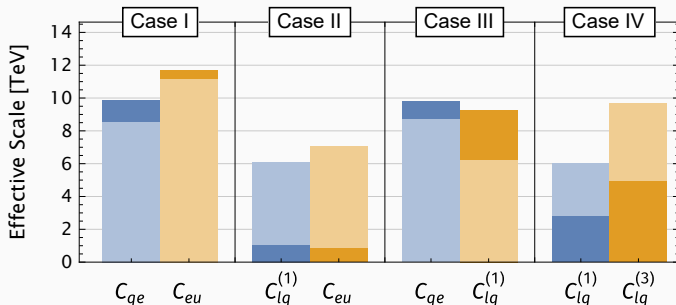


CASE IV $C_{lq}^{(1)}$ and $C_{lq}^{(3)}$

- no flat directions at linear order, strong correlation between $C_{lq}^{(1)}$ and $C_{lq}^{(3)}$
- Supplementing AFB is unable to reduce such correlation
- Quadratic contributions improve the combined fit significantly



EFFECTIVE SCALE



- Effective scales M from 68% bounds (choosing $g = 1, \Lambda = 4$ TeV)

$$\frac{C}{\Lambda^2} \sim \frac{g^2}{M^2}$$

- lighter bars: quadratic included
- darker bars: only linear terms
- improvement from quadratic terms in case II & IV (where AFB didn't help), but not I & III

CONCLUSIONS

- Combining measurements of $d\sigma/dm$ and AFB in neutral-current Drell-Yan
- Fits to the four-fermion sector of the SMEFT at dimension-6
- In some cases, AFB helps to break degeneracies in $d\sigma/dm$, greatly improving the fits
- In other cases, AFB does not help
- Linear & quadratic fits agree when AFB can break degeneracies
- Significant differences btw. linear & quadratic fits when AFB cannot break degeneracies

Thanks for your attention!

Backup

TWO PRESCRIPTIONS OF AFB quark direction

- quark direction approximated w/ dilepton momentum

$$\cos \theta_R = \frac{|Q^z|}{Q^z} \cos \theta^*.$$

We denote this prescription as A_{FB}^* .

Asymmetry diluted when quark direction not aligned with dilepton direction
(e.g. small $|y|$ region)

- using Monte-Carlo as template, identify quark direction at parton level,
denoted by A_{FB} (the "true" AFB) [Tumasyan et al. 2022](#); [Accomando et al. 2016](#)
 - Gluon initiated processes: In our calculations, we assign quark direction that's consistent with the cancellation of collinear singularities
i.e. $g\bar{q}$: quark direction set to gluon direction

UNCERTAINTIES

- No correlation between the data sets
- Data set I: experimental uncertainties provided by ATLAS, including full statistical and systematic errors
- Rest of the data sets: no correlated systematic error provided
 - Data set II: assume no correlation between different bins & channels
 - Data set III: assume no correlation between different bins, it's tested that the correlations have little effect
 - Data set IV: assume no correlation between different bins, same as data set III
- Theoretical uncertainties:
 - correlated PDF errors across bins and data sets
 - uncorrelated scale uncertainties
 - NNLO QCD corrections less than 2% for most bins
 - electroweak corrections as much as 10% for high $m_{\ell\ell}$ bins
 - Scale choice: $\mu_0 = m_{\ell\ell}$ for data set I, II, III
 - Data set IV: Use $\mu_0 = H_T^5$ as the central value. Calculate both $\mu_0 = m_{\ell\ell}$ & $\mu_0 = H_T$ along with their 6 scale variations, then take the envelope.

EVENT NUMBERS IN DATA SET II

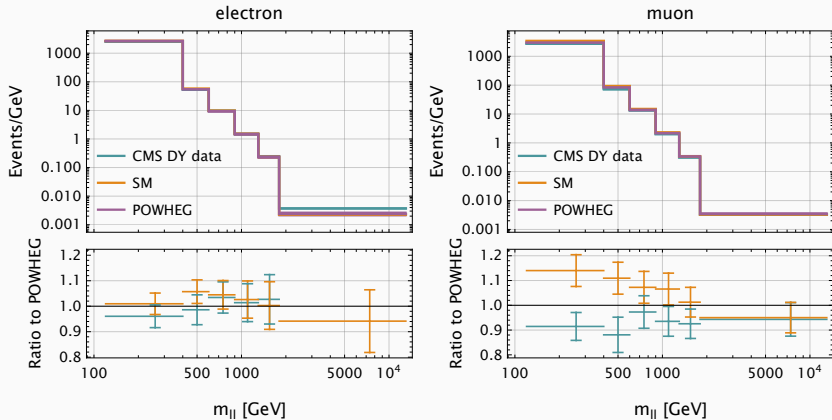


Figure: Event yields in the electron (left) and muon (right) channels for the 13 TeV data set II. The green lines show the observed total event yields minus all non-Drell-Yan backgrounds. The orange lines show our SM predictions with electroweak Sudakov corrections. The purple line shows the POWHEG estimate for the Drell-Yan background. The lower inset shows the ratio to the Drell-Yan background estimations in Ref. Sirunyan et al. 2021. The error bars represent uncertainties from the POWHEG estimates.

SCALE CHOICE W/ DATA SET IV

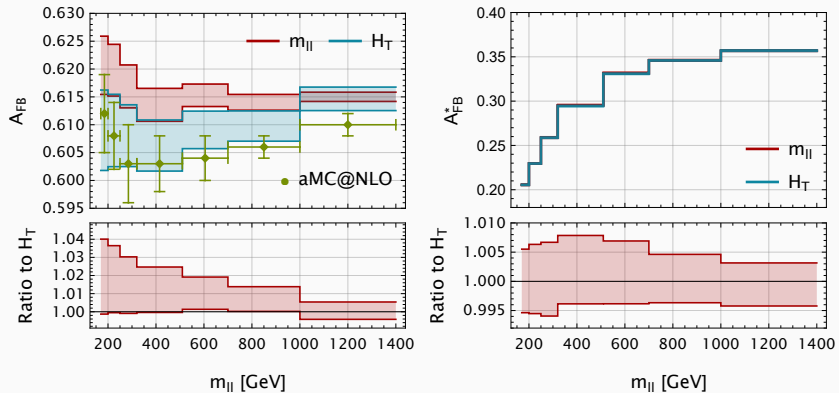


Figure: Left panel: The “true” forward-backward asymmetry A_{FB} for data set IV with dynamic scale $\mu_0 = m_{||}$ (red) and $\mu_0 = H_T$ (blue). The bands represent the range of scale variation ($1/2 \leq \mu_{R,F}/\mu_0 \leq 2$, $1/2 \leq \mu_R/\mu_F \leq 2$) for both scale choices. The aMC@NLO simulation in Ref. Tumasyan et al. 2022 is shown by the green points. Right panel: the same comparison for A_{FB}^* .